

Vibration Analysis of Free Rectangular Plates Constrained by Translational Edge Springs

Yoshihiro Narita^{a,*}

^aHokkaido University (Professor Emeritus), N-13, W-8, Sapporo, Japan. Email: ynarita1951@gmail.com

Abstract

This paper aims to present comprehensive lists of accurate natural frequencies of isotropic thin free rectangular plates constrained only by translational springs distributed uniformly on the edges. Analytical and numerical approaches are employed to study the free vibration of the plates. The first approach is an extension of the Ritz method, and the second approach is the finite element method coded by the author. Numerical examples cover rectangular plates from totally free to totally simply supported plates on all edges. Convergence and comparison studies are made to establish the accuracy of these solutions. Nine numerical examples are presented in terms of different elastic constraints, and the lowest six frequency parameters are provided in the examples with different aspect ratios.

Keywords: Free vibration; rectangular plate; translational spring; natural frequency; mode shape

1. Introduction

Flat metal and composite plates are basic structural components in modern technology, and vibration analysis of such plates has been one of the most important technical issues in engineering. On the topic, a famous monograph [1] has covered the literature on vibration of plates in various geometry, and Gorman [2] wrote a textbook by using the superposition method. Among various plate shapes, rectangular plate is the most common shape and the natural frequencies of isotropic rectangular plates were summarized [3] in 1973 for all possible twenty-one combinations of boundary conditions and five aspect ratios. The present author published papers on rectangular plates under classical boundary conditions [4], [5] such as free, simply supported and clamped edges. These ideal boundary conditions are mathematically well defined.

In practice, however, the plate edges are recognized to be elastically constrained in the intermediate state between free and simply supported condition or between simply supported and clamped condition. Some decades ago, Laura and his coworkers have worked on vibration of simply supported rectangular plates constrained against rotation along all edges [6]–[9]. Bapat and Venkatramani [10] simulated the classical edge conditions by finite elastic restraints, and Gorman [11] presented a study on vibration of rectangular plates resting on symmetrically-distributed uniform elastic edge supports. Grossi and Bhat [12] presented natural frequencies of edge restrained tapered rectangular plates.

In the 2000's, Li and Yu [13] proposed a simple formula for natural frequencies of plates with uniformly restrained edges, and Li and others [14] presented a series solution for rectangular plates with general elastic boundary supports. Eftekhari and Jafari [15] used a variational approach for vibration of variable thickness plates with elastic edges, and Ahmadian and Esfandiar [16] attempted to identify the elastic boundary condition.

More recently in the 2020's, Wan [17] presented vibration analysis of rectangular plates with elastic boundary conditions, and Zhang and others [18] studied rectangular plates with two adjacent edges rotationally-restrained by using finite Fourier integral transform method. Leng and others [19] proposed analytical solutions by using the Fourier series method. Thus, this topic on vibration of rectangular plates with elastic edge condition still attracts attention of researchers. Numerical results are however limited to simply supported plates with rotational springs, and the lack in frequency data is

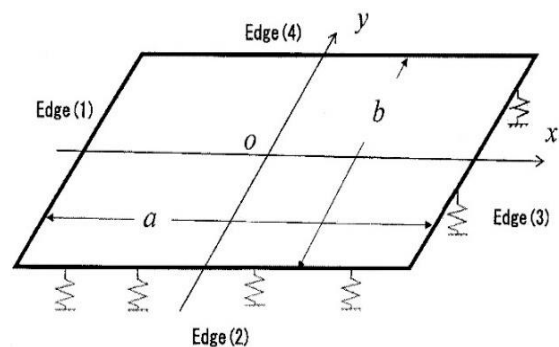


Figure 1. Rectangular plate with uniform translational springs on the edges and the coordinate system

*Corresponding author.
Hokkaido University, N-13, W-8, Sapporo
Japan

obvious for free plates elastically constrained only by translational springs. This paper is intended to fill this gap and serves for structural design by considering plates loosely coupled with edges.

2. Methods of Analysis

2.1. Extension of Ritz method to inclusion of edge springs

A previous solution is extended here as in Refs. [4], [5] based on the method of Ritz under the classical thin plate theory. This analysis-based solution has a low computational cost and easiness in varying combinations in boundary conditions, as compared to numerical methods such as the finite element method. Figure 1 shows a geometry of rectangular plate and the coordinate system, and the dimension of the plate is given by $a \times b \times h$ (thickness). The relation between stress and strain in isotropic plate is

$$\begin{Bmatrix} \sigma_x \\ \sigma_y \\ \tau_{xy} \end{Bmatrix} = \begin{bmatrix} Q_{11} & Q_{12} & 0 \\ Q_{12} & Q_{22} & 0 \\ 0 & 0 & Q_{66} \end{bmatrix} \begin{Bmatrix} \varepsilon_x \\ \varepsilon_y \\ \gamma_{xy} \end{Bmatrix} \quad (1)$$

with the matrix elements given by

$$Q_{11} = Q_{22} = \frac{E}{1-\nu^2}, Q_{12} = \nu Q_{11}, Q_{66} = G = \frac{E}{2(1+\nu)} \quad (2)$$

where E is Young's modulus, G is a shear modulus and ν is a Poisson's ratio. When Eq.(1) is integrated through the thickness after multiplying a thickness coordinate z , one gets moment resultants in terms of curvature

$$\begin{Bmatrix} M_x \\ M_y \\ M_{xy} \end{Bmatrix} = \begin{bmatrix} D_{11} & D_{12} & 0 \\ D_{12} & D_{22} & 0 \\ 0 & 0 & D_{66} \end{bmatrix} \begin{Bmatrix} \kappa_x \\ \kappa_y \\ \kappa_{xy} \end{Bmatrix} \quad (3)$$

If one considers the small amplitude (linear) free vibration of plate, the deflection w may be written by

$$w(x, y, t) = W(x, y) \sin \omega t \quad (4)$$

where W is the amplitude and ω is a radian frequency of the plate. Then, the maximum strain energy due to the bending is expressed by

$$U_{\max} = \frac{1}{2} \iint_A \{\kappa\}^T \begin{bmatrix} D_{11} & D_{12} & 0 \\ D_{12} & D_{22} & 0 \\ 0 & 0 & D_{66} \end{bmatrix} \{\kappa\} dA \quad (5)$$

where the D_{ij} are the bending stiffnesses and $\{\kappa\}$ is a curvature vector

$$\{\kappa\} = \left\{ -\frac{\partial^2 W}{\partial x^2} \quad -\frac{\partial^2 W}{\partial y^2} \quad -2\frac{\partial^2 W}{\partial x \partial y} \right\}^T \quad (6)$$

The maximum kinetic energy is also given by

$$T_{\max} = \frac{1}{2} \rho h \omega^2 \iint_A W^2 dA \quad (7)$$

where ρ [kg/m^3] is the mass per unit volume.

For the sake of simplicity, non-dimensional quantities are introduced as

$$\begin{aligned} \xi &= \frac{2x}{a}, \eta = \frac{2y}{b} \quad (\text{non-dimensional coordinates}), \\ \alpha &= \frac{a}{b} \quad (\text{aspect ratio}), \quad d_{ij} = \frac{D_{ij}}{D} \\ D &= \frac{Eh^3}{12(1-\nu^2)} \quad (\text{reference stiffness}) \\ \Omega &= \omega a^2 \sqrt{\frac{\rho h}{D}} \quad (\text{frequency parameter}) \end{aligned} \quad (8)$$

Next, we consider the energy stored in the elastic restraints (translational elastic springs). The energy equation is written as

$$\begin{aligned} U_t &= \\ &\frac{1}{2} \left\{ \int_{-b/2}^{b/2} k_{t1} w^2 \left(-\frac{a}{2}, y \right) dy + \int_{-a/2}^{a/2} k_{t2} w^2 \left(x, -\frac{b}{2} \right) dx \right. \\ &\quad \left. + \int_{-b/2}^{b/2} k_{t3} w^2 \left(+\frac{a}{2}, y \right) dy + \int_{-a/2}^{a/2} k_{t4} w^2 \left(x, +\frac{b}{2} \right) dx \right\} \quad (9) \end{aligned}$$

by where k_{ti} ($i=1,2,3,4$) are stiffness of translational springs in unit [N/m^2] per unit edge length. This energy is added to the elastic bending energy (5).

The next step in the Ritz method is to assume the amplitude as

$$W(\xi, \eta) = \sum_{m=0}^{M-1} \sum_{n=0}^{N-1} A_{mn} X_m(\xi) Y_n(\eta) \quad (10)$$

where A_{mn} are unknown coefficients, and $X_m(\xi)$ and $Y_n(\eta)$ are the functions modified so that any kinematical boundary conditions are satisfied at the edges [4], [5].

After substituting Eq.(10) into these energies, the stationary value is obtained by

$$\frac{\partial}{\partial A_{\bar{m}\bar{n}}} \left\{ T_{\max} - (U_{\max} + U_{t,\max}) \right\} = 0 \quad (\bar{m} = 0, 1, 2, \dots, (M-1); \bar{n} = 0, 1, 2, \dots, (N-1)) \quad (11)$$

Then the eigenvalue equation that contains a frequency parameter Ω is derived as

$$\begin{aligned} &\sum_{m=0}^{M-1} \sum_{n=0}^{N-1} \left[d_{11} I^{(2200)} + \alpha^2 d_{12} (I^{(2002)} + I^{(0220)}) + \alpha^4 d_{22} I^{(0022)} \right. \\ &\quad \left. + 4\alpha^2 d_{66} I^{(1111)} + (\text{Spring term}) - \Omega^2 I^{(0000)} \right]_{\bar{m}\bar{n}\bar{m}\bar{n}} \cdot A_{\bar{m}\bar{n}} = 0 \quad (\bar{m} = 0, 1, 2, \dots, (M-1); \bar{n} = 0, 1, 2, \dots, (N-1)) \quad (12) \end{aligned}$$

where an integral I is the products

$$I_{mmnn}^{(pqrs)} = \phi_{mm}^{(pq)} \cdot \phi_{nn}^{(rs)} \quad (13)$$

of the two integrals defined by

$$\phi_{mm}^{(pq)} = \int_{-1}^1 \frac{\partial^{(p)} X_m}{\partial \xi^{(p)}} \frac{\partial^{(q)} X_m}{\partial \xi^{(q)}} d\xi \quad (14)$$

and (Spring term) is the line integral along an edge. Equation (12) is a set of linear simultaneous equations in terms of the coefficients A_{mn} , and the eigenvalues Ω may be extracted by using existing computer subroutines.

The analytical procedure developed thus far is a standard routine of a Ritz method, and the modification is explained next so as to incorporate arbitrary edge conditions into the amplitude $W(\xi, \eta)$. In the traditional approach using the beam functions for $X_m(\xi)$ and $Y_n(\eta)$, many different products of regular and hyper trigonometric functions exist for arbitrary conditions and it is difficult to make a unified subroutine to calculate all kinds of integrals.

The present approach uses simple polynomials

$$X_m(\xi) = \xi^m, \quad Y_n(\eta) = \eta^n \quad (15)$$

to represent freely supported plates as a base, and the integrals (13) can be exactly calculated.

2.2. Finite element formulation of edge spring

A finite element is newly developed to include the effect of translational springs distributed along the edges, and the finite element code (FEM code) is made to compare the result with the Ritz solution to establish accuracy of both methods. Formulation of plate bending element and kinetic element are already explained in Ref. [20]. Here only formulation of the edge spring element is shown.

The deflection inside the element including boundary is assumed by

$$W(x, y, t) = \{P\} \{\alpha\} \sin \omega t \quad (16)$$

where $\{P\}$ and $\{\alpha\}$ are (T: transpose)

$$\{P\} = \{1, x, y, x^2, xy, y^2, x^3, x^2y, xy^2, y^3, x^3y, xy^3\} \quad (17)$$

$$\{\alpha\} = \{\alpha_1, \alpha_2, \alpha_3, \alpha_4, \alpha_5, \alpha_6, \alpha_7, \alpha_8, \alpha_9, \alpha_{10}, \alpha_{11}, \alpha_{12}\}^T \quad (18)$$

The displacement at node i is defined as

$$\{\delta_i\} = \{W_i, (\partial W / \partial x)_i, (\partial W / \partial y)_i\}^T \quad (19)$$

and the displacements of four nodes labelled as i, j, k and l in a rectangular element can be expressed as

$$\{\delta_e\} = \{\delta_i \quad \delta_j \quad \delta_k \quad \delta_l\}^T \quad (20)$$

Using $[C]$ which is obtained by substituting Eq.(16) into the four sets of node coordinates, W is transformed as

$$W(x, y) = \{P\} [C]^{-1} \{\delta_e\} \quad (21)$$

For example, when the translational spring is distributed along Edge(2) or Edge(4) at $y = \bar{y}$, equation (20) is substituted into the second or fourth term of Eq.(9) and

$$\frac{1}{2} \int_{-a/2}^{a/2} k_{ii} W^2(x, \bar{y}) dx = \frac{1}{2} \{\delta_e\}^T [K_{ii}] \{\delta_e\} \quad (22)$$

($i=2,4$) is obtained, where $[K_{ii}]$ is a finite element of translational edge spring

$$[K_{ii}] = k_{ii} [C^{-1}]^T \left(\int \{P(x, \bar{y})\}^T P(x, \bar{y}) dx \right) [C^{-1}] \quad (23)$$

with $P(x, \bar{y})$ being a function of (x, y) at fixed $\bar{y} = -b/2$ or $\bar{y} = b/2$ for Edge(2) and Edge (4), respectively. Spring finite elements along Edge(1) and Edge(3) can be formulated in the same manner.

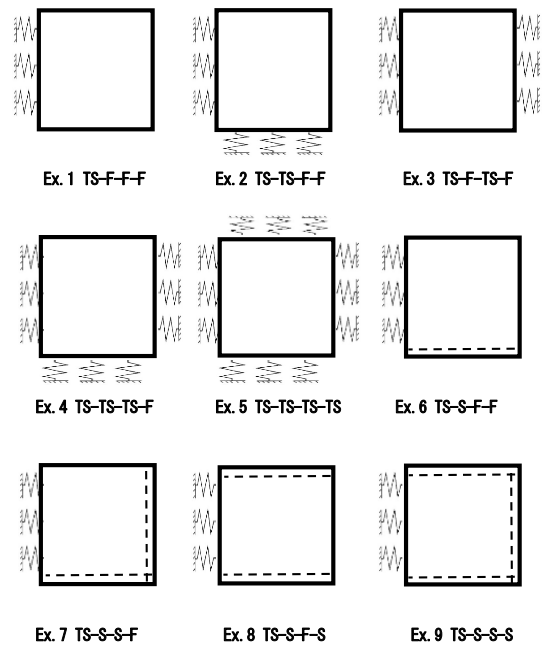


Figure 2. Numerical examples Ex.1-Ex.9 (TS: edge with translational spring, F: free edge, S: simple supported edge)

Table 1. Convergence of the present (a) Ritz solution and (b)FEM solution for square plates elastically supported at one edge (Ex.1)

k_{11}^*		Ω_1	Ω_2	Ω_3	Ω_4	Ω_5
(a) Present Ritz solution						
100	6 × 6	5.557	12.63	19.71	23.59	32.19
	8 × 8	5.557	12.62	19.71	23.41	31.71
	10 × 10	5.556	12.62	19.71	23.41	31.70
10000	6 × 6	6.604	14.89	25.30	26.18	48.94
	8 × 8	6.602	14.86	25.24	25.92	48.02
	10 × 10	6.601	14.86	25.24	25.92	48.01
(b) Present FEM solution						
100	10 × 10	5.558	12.63	19.71	23.41	31.73
	15 × 15	5.556	12.63	19.71	23.41	31.72
	20 × 20	5.555	12.63	19.71	23.41	31.71
10000	10 × 10	6.604	14.88	25.24	25.91	48.00
	15 × 15	6.602	14.87	25.24	25.91	48.00
	20 × 20	6.600	14.87	25.24	25.91	48.00

3. Numerical Examples and Discussions

3.1. Convergence and comparison of the solution

The plate is assumed to be made of isotropic material, and Young's modulus E and Poisson's ratio ν are included in the dimensionless frequency parameters Ω in Eq.(8). Poisson's ratio $\nu=0.3$ is used throughout in the paper.

Figure 2 illustrates numerical examples Ex.1-Ex.9 with different degree of elastic constraints by translational springs (such edge is denoted by "TS"). When they have multiple translational springs on the edges, it is assumed that all the springs have the same degree of constraint

$$k_t^* = k_{t1} \left(\frac{a^3}{D} \right) = k_{t2} \left(\frac{a^3}{D} \right) = k_{t3} \left(\frac{a^3}{D} \right) = k_{t4} \left(\frac{a^3}{D} \right) \quad (24)$$

in the calculation, although they can be different.

Ex.1 is a free plate with only one edge constrained by a translational spring. This plate shows three rigid body motions (RBM) for $k_t^*=0$ (i.e., F-F-F-F plate), which are one out-of-plane translational motion and two rotational motions about two coordinate axes. These RBM's are common at $k_t^*=0$ in Ex.1-Ex.5. When k_t^* becomes non-zero positive value and increased, Ex.1 starts to show only one rotational RBG but RBM's of Ex.2-Ex.5 disappear. Ex.6-Ex.9 have a translational spring on one edge and plural simply supported edges. Thus, Ex.1-Ex.9 cover most cases of plates with less edge constraints than an entirely simply supported plate.

Table 1 summarizes convergence study for the present (a) Ritz solution and (b)FEM solution for square plates in Ex.1. For both types of solutions, $k_t^*=100$ and 10000 are assumed. (a) Ritz solution uses the number of series terms 6×6 , 8×8 , 10×10 in Eq.(10), and converge within four significant figures in most cases. In (b) FEM solution, the number of finite elements in x and y directions is increased as 10×10 , 15×15 , 20×20 , and they also exhibit fast convergence in the four significant figures.

Table 2. Frequency parameters of square plates (Ex.1 TS-F-F-F, $\nu=0.3$)

k_t^*		Ω_1	Ω_2	Ω_3	Ω_4	Ω_5
0	Ritz	13.47	19.60	24.27	34.80	34.80
	FEM	13.47	19.60	24.28	34.80	34.80
1	Ritz	0.990	1.990	13.57	19.66	24.32
	FEM	0.999	1.990	13.57	19.67	24.33
10	Ritz	2.886	6.001	14.45	20.26	24.82
	FEM	2.886	6.001	14.45	20.26	24.82
100	Ritz	5.556	12.62	19.71	23.41	31.70
	FEM	5.555	12.63	19.71	23.41	31.71
10000	Ritz	6.601	14.86	25.24	25.92	48.01
	FEM	6.600	14.87	25.24	25.92	48.01
infinity	Ritz	6.643	14.90	25.38	26.00	48.45
	FEM	6.643	14.91	25.38	26.00	48.46

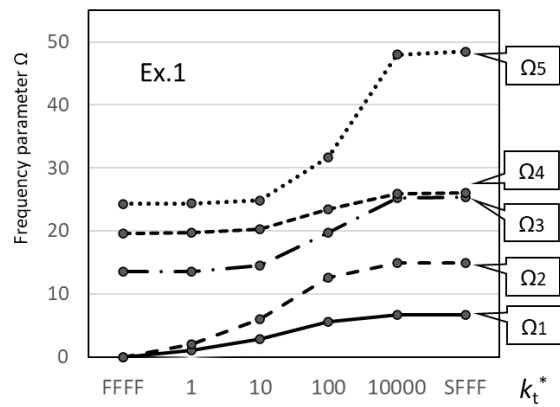


Figure 3. Variation of frequency parameters of square plate Versus spring stiffness (Ex.1)

It is noted that both sets of results by the Ritz and FEM solutions agree very well. In previous references, a few papers [14,15] presented some results of plates with non-zero constraints in both translational and rotational springs, but it seems that no results are available for the present case (i.e., free plate with only translational spring). In the following numerical results, the 10×10 term in (a) Ritz solution and the 20×20 element in (b) FEM are used.

3.2. Frequency parameters of square plates

Tables 2-10 present the lowest five frequency parameters for Ex.1-Ex.9, respectively, versus the increasing degree of translational springs as $k_t^*=0$ (free edge), 1, 10, 100, 10000. In the limiting case of $k_t^*=\infty$ (infinity), the frequency values are available from Ref.[5] by replacing $k_t^*=\infty$ (TS) by simple support (S). It is seen in common that the frequencies are monotonically increasing, as TS edge starts from free edge $k_t^*=0$ to strongly constrained edge $k_t^*=10000=10^4$, and this edge ($k_t^*=10^4$) practically gives the similar frequency value as the simple support.

As previously stated, there are three RBM's (rigid body motion) for F-F-F-F plate in Ex.1-5 (Tables 2-6), one RBM in Ex.6 (Table 7) and zero RBM in Ex.7-9 (Tables 8-10) for $k_t^*=0$. Although such RBM's disappear as the stiffness is increased, one RBM still remains in Ex.1 due to one rotational RBD along one edge support.

Table 3. Frequency parameters of square plates (Ex.2 TS-TS-F-F, $\nu=0.3$)

k_t^*		Ω_1	Ω_2	Ω_3	Ω_4	Ω_5
0	Ritz	13.47	19.60	24.27	34.80	34.80
	F-F-F-F					
1	Ritz	0.5858	1.990	2.363	13.67	19.73
10	Ritz	1.640	6.008	7.108	15.37	20.94
100	Ritz	2.887	13.18	15.29	24.56	31.03
10000	Ritz	3.348	17.18	19.22	37.72	50.74
infinity	Ritz	3.368	17.32	19.29	38.21	51.04
S-S-F-F						

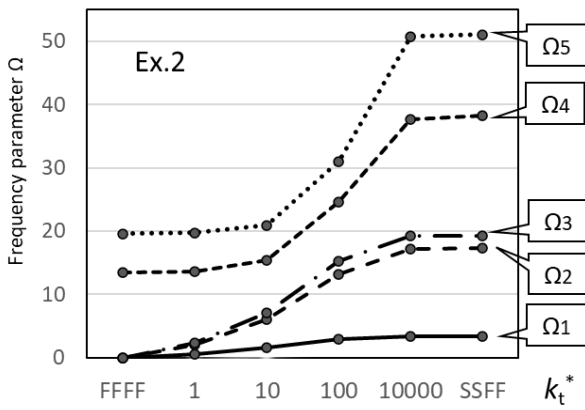


Figure 4. Variation of frequency parameters of square plate versus spring stiffness (Ex.2)

Table 4. Frequency parameters of square plates (Ex.3 TS-F-TS-F, $\nu=0.3$)

k_t^*		Ω_1	Ω_2	Ω_3	Ω_4	Ω_5
0	Ritz	13.47	19.60	24.27	34.80	34.80
F-F-F-F						
1	Ritz	1.402	1.410	2.447	13.67	19.73
10	Ritz	4.104	4.326	7.650	15.34	20.82
100	Ritz	8.063	10.73	21.64	25.25	25.68
10000	Ritz	9.603	15.94	36.14	38.60	46.07
infinity	Ritz	9.631	16.13	36.73	38.95	46.74
S-F-S-F						

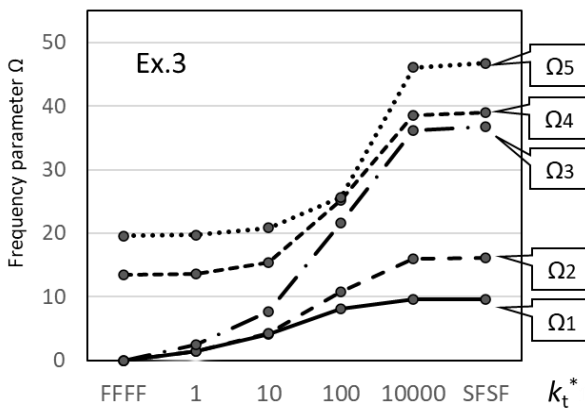


Figure 5. Variation of frequency parameters of square plate versus spring stiffness (Ex.3)

Table 5. Frequency parameters of square plates (Ex.4 TS-TS-TS-F, $\nu=0.3$)

k_t^*		Ω_1	Ω_2	Ω_3	Ω_4	Ω_5
0	Ritz	13.47	19.60	24.27	34.80	34.80
F-F-F-F						
1	Ritz	1.403	2.439	2.640	13.77	19.80
10	Ritz	4.163	7.435	8.185	16.21	21.51
100	Ritz	8.872	17.45	22.41	29.46	33.43
10000	Ritz	11.60	27.34	40.75	57.78	60.80
infinity	Ritz	11.68	27.76	41.20	59.07	61.86
S-S-S-F						

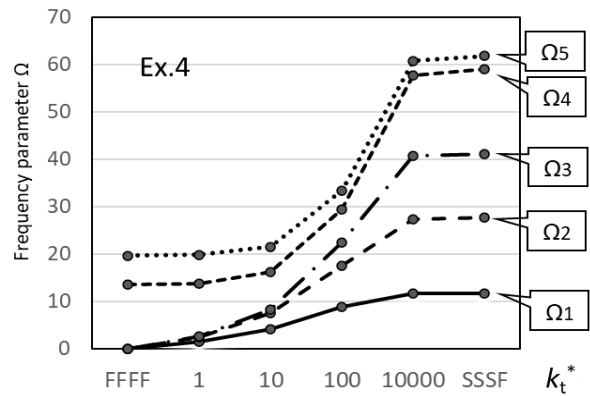


Figure 6. Variation of frequency parameters of square plate versus spring stiffness (Ex.4)

Table 6. Frequency parameters of square plates (Ex.5 TS-TS-TS-TS, $\nu=0.3$)

k_t^*		Ω_1	Ω_2	Ω_3	Ω_4	Ω_5
0	Ritz	13.47	19.60	24.27	34.80	34.80
F-F-F-F						
1	Ritz	1.986	2.825	2.825	13.87	19.86
10	Ritz	5.928	8.813	8.813	17.01	22.10
100	Ritz	13.00	24.66	24.66	33.54	37.00
10000	Ritz	19.50	48.47	48.47	76.43	95.96
infinity	Ritz	19.74	49.35	49.35	78.96	98.70
S-S-S-S						

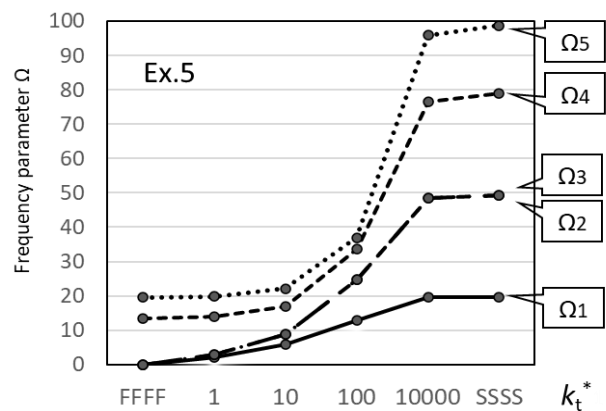


Figure 7. Variation of frequency parameters of square plate versus spring stiffness (Ex.5)

In the first five examples of Ex.1-Ex.5 where three RBM's are observed at $k_t^*=0$, Tables 2-6 summarize values of the lowest five frequency parameters (zero frequencies at $k_t^*=0$ are excluded), and to avoid misunderstanding, Figures 3-7 are accompanied to demonstrate continuous variation of frequency parameters from $k_t^*=0$ to $k_t^*=\infty$ (infinity).

In Table 2, for example, frequency values in Ex.1 are presented and they show the good agreement again between the present Ritz and FEM solutions. The discrepancy between both solutions is less than 0.05 percent, except for only one case of 0.9 percent. Variation of the frequency parameters is plotted in continuous (piece-wise linear) lines in Fig.3, and in this case two RBM's become non-zero frequencies with the increase in

stiffness. Similarly in Tables 3-6 list up the frequency parameters obtained by the Ritz solution in Ex.2-Ex.5, respectively. There are three RBM's at $k_t^*=0$. They disappear as the stiffness is added, and such modes have non-zero frequencies. Generally speaking, the frequency values at $k_t^*=10000$ and $k_t^*=(\text{infinity})$ give almost same values but slight difference occurs as more springs are added (i.e., Ex.1→Ex.5).

Table 7. Frequency parameters of square plates (Ex.6 TS-S-F-F, $\nu=0.3$)

k_t^*		Ω_1	Ω_2	Ω_3	Ω_4	Ω_5
0	Ritz	6.643	14.90	25.38	26.00	48.45
	F-S-F-F FEM	6.643	14.91	25.38	26.00	48.46
1	Ritz	0.964	6.864	14.94	25.43	26.07
	FEM	0.975	6.866	14.95	25.43	26.07
10	Ritz	2.341	8.656	15.29	25.91	26.76
	FEM	2.341	8.656	15.30	25.91	26.76
100	Ritz	3.167	14.66	17.28	29.73	33.82
	FEM	3.164	14.66	17.28	29.72	33.83
10000	Ritz	3.360	17.25	19.27	37.98	50.88
	FEM	3.361	17.25	19.26	37.94	50.90
infinity	Ritz	3.368	17.32	19.29	38.21	51.04
S-S-F-F	FEM	3.366	17.32	19.29	38.17	51.06

Table 8. Frequency parameters of square plates (Ex.7 TS-S-S-F, $\nu=0.3$)

k_t^*		Ω_1	Ω_2	Ω_3	Ω_4	Ω_5
0	Ritz	3.368	17.32	19.29	38.21	51.04
	F-S-S-F					
1	Ritz	4.457	17.88	19.92	38.73	51.50
10	Ritz	5.916	18.33	20.09	38.67	51.39
100	Ritz	10.17	22.59	27.89	42.57	54.11
10000	Ritz	11.66	27.61	40.99	58.58	61.56
infinity	Ritz	11.68	27.76	41.20	59.07	61.86
S-S-S-F						

Table 9. Frequency parameters of square plates (Ex.8 TS-S-F-S, $\nu=0.3$)

k_t^*		Ω_1	Ω_2	Ω_3	Ω_4	Ω_5
0	Ritz	9.631	16.13	36.73	38.95	46.74
	F-S-F-S					
1	Ritz	9.693	16.23	36.78	38.96	46.77
10	Ritz	10.13	17.03	37.23	39.11	47.05
100	Ritz	11.25	22.28	39.99	42.02	49.60
10000	Ritz	11.68	27.68	41.17	58.83	61.47
infinity	Ritz	11.68	27.76	41.20	59.07	61.86
S-S-F-S						

Table 10. Frequency parameters of square plates (Ex.9 TS-S-S-S, $\nu=0.3$)

k_t^*		Ω_1	Ω_2	Ω_3	Ω_4	Ω_5
0	Ritz	11.68	27.76	41.20	59.07	61.86
	F-S-S-S FEM	11.69	27.72	41.21	58.93	61.74
1	Ritz	11.81	27.82	41.23	59.09	61.89
	FEM	11.81	27.79	41.25	58.95	61.77
10	Ritz	12.79	28.43	41.55	59.34	62.19
	FEM	12.79	28.40	41.56	59.20	62.06
100	Ritz	16.93	34.22	43.91	61.83	65.39
	FEM	16.91	34.19	43.89	61.68	65.27
10000	Ritz	19.70	49.09	49.23	78.39	97.67
	FEM	19.68	48.99	49.13	77.98	97.44
infinity	Ritz	19.74	49.35	49.35	78.96	98.70
S-S-S-S	FEM	19.71	49.24	49.24	78.54	98.47

Tables 7-10 list up similar sets of frequency parameters for square plates with one or more simply supported edges (Ex.6-Ex.9). Table 7 (Ex.6) gives the frequency parameter of square plates with elastic constraints between F-S-F-F (one RBM) and S-S-F-F, and once again the good agreement is assessed by using both present Ritz and FEM solutions. The maximum discrepancy is 1.1 percent and most of them are under 0.5 percent. Table 8 (Ex.7) gives sets of frequencies for square plates with two adjacent simple supported edges and elastic constraints between F-S-S-F and S-S-S-F, and Table 9 (Ex.8) does sets of frequencies for square plates with the opposite edges simply supported and one edge with elastic constraint between F-S-F-S and S-S-F-S. Table 10 (Ex.9) presents a set of frequencies of square plate with three edges simply supported and one elastic edge. In the limiting case of $k_t^*=\text{infinity}$, the frequency parameters are obtained for S-S-S-S plate. The maximum difference is 0.5 percent in Table 10.

Thus, almost all the cases are summarized for square plates constrained by translational springs only, namely the natural frequencies are tabulated for the first time for square plates with elastic edge constraints less or equal to totally simply supported plates.

3.3. Frequency parameters of rectangular plates

For rectangular plates with different aspect ratios, the lowest five frequencies are calculated in Ex.1-Ex.5. Aspect ratio is taken at $a/b=2/3$ and $a/b=1.5$ in Table 11 and 12, respectively. As in the square plate, the plates are totally free (F-F-F-F) at $k_t^*=0$. These are simply supported at one edge (Ex.1), two edges (Ex.2, 3), three edges (Ex.4) and four edges (Ex.5) in the limiting value of stiffness ($k_t^*=\text{infinity}$), and among them, the exact solutions are available for Ex.3,4 and 5 where the opposite edges are simply supported (Levy type solution).

Table 11. Frequency parameter of rectangular plates
($a/b=2/3$, Ex.1-Ex.5, $\nu=0.3$)

k_t^*	Ω_1	Ω_2	Ω_3	Ω_4	Ω_5
Ex.1					
0					
F-F-F-F	8.931	9.517	20.60	22.18	25.65
1	0.9792	1.990	9.093	9.576	20.67
10	2.621	5.997	10.05	10.45	21.25
100	4.062	11.39	13.36	16.40	25.56
10000	4.462	12.89	15.55	20.17	30.33
infinity					
S-F-F-F	4.477	12.94	15.57	20.25	30.39
Ex.2					
0					
F-F-F-F	8.931	9.517	20.60	22.18	25.65
1	0.522	1.756	2.189	9.185	9.718
10	1.341	4.865	6.490	11.17	11.53
100	2.024	8.167	13.68	18.69	20.32
10000	2.225	9.498	16.63	24.42	26.82
infinity					
S-S-F-F	2.233	9.539	16.68	24.54	26.99
Ex.3					
0					
F-F-F-F	8.931	9.517	20.60	22.18	25.65
1	1.401	1.407	2.447	9.248	9.635
10	4.104	4.252	7.652	10.60	11.67
100	8.105	9.652	15.62	21.67	23.35
10000	9.672	12.89	22.69	38.77	39.86
infinity					
S-F-S-F	9.698	12.98	22.95	39.11	40.36
Ex.4					
0					
F-F-F-F	8.931	9.517	20.60	22.18	25.65
1	1.403	2.137	2.576	9.339	9.775
10	4.145	6.164	7.983	11.95	12.36
100	8.561	12.67	22.06	22.18	25.53
10000	10.63	18.13	33.29	39.76	47.73
infinity					
S-S-S-F	10.67	18.30	33.70	40.13	48.41
Ex.5					
0					
F-F-F-F	8.931	9.517	20.60	22.18	25.65
1	1.802	2.440	2.703	9.429	9.910
10	5.153	7.465	8.407	12.96	13.00
100	10.46	17.88	23.23	27.20	28.22
10000	14.16	27.12	43.35	48.70	55.93
infinity					
S-S-S-S	14.26	27.42	43.86	49.35	57.02

Table 12. Frequency parameter of rectangular plates
($a/b=1.5$, Ex.1-Ex.5, $\nu=0.3$)

k_t^*	Ω_1	Ω_2	Ω_3	Ω_4	Ω_5
Ex.1					
0					
F-F-F-F	20.10	21.41	46.35	49.91	57.71
1	0.9944	1.989	20.16	21.51	46.38
10	3.030	6.001	20.71	22.39	46.72
100	7.116	12.65	24.93	31.04	50.10
10000	9.741	14.85	33.60	47.74	54.53
infinity					
S-F-F-F	9.846	14.89	33.91	47.95	54.78
Ex.2					
0					
F-F-F-F	20.10	21.41	46.35	49.91	57.71
1	0.6536	2.174	2.696	20.27	21.55
10	1.916	6.607	8.353	21.75	22.75
100	3.935	15.02	22.42	31.53	33.62
10000	4.979	21.22	37.18	54.47	59.60
infinity					
S-S-F-F	5.026	21.46	37.53	55.22	60.74
Ex.3					
0					
F-F-F-F	20.10	21.41	46.35	49.91	57.71
1	1.400	1.410	2.446	20.22	21.60
10	4.103	4.389	7.649	21.30	23.26
100	8.041	11.96	21.61	29.09	36.37
10000	9.528	21.18	38.37	53.69	64.59
infinity					
S-F-S-F	9.559	21.62	38.72	54.84	65.79
Ex.4					
0					
F-F-F-F	20.10	21.41	46.35	49.91	57.71
1	1.405	2.734	2.823	20.33	21.64
10	4.181	8.483	8.801	22.31	23.60
100	9.306	23.08	24.40	35.84	37.88
10000	13.54	42.94	46.80	78.56	90.57
infinity					
S-S-S-F	13.71	43.57	47.86	81.48	92.69
Ex.5					
0					
F-F-F-F	20.10	21.41	46.35	49.91	57.71
1	2.228	2.997	3.314	20.43	21.68
10	6.807	9.383	10.43	23.24	23.95
100	17.19	26.94	31.48	39.93	40.95
10000	31.43	59.74	95.06	106.5	120.9
infinity					
S-S-S-S	32.08	61.68	98.70	111.0	128.3

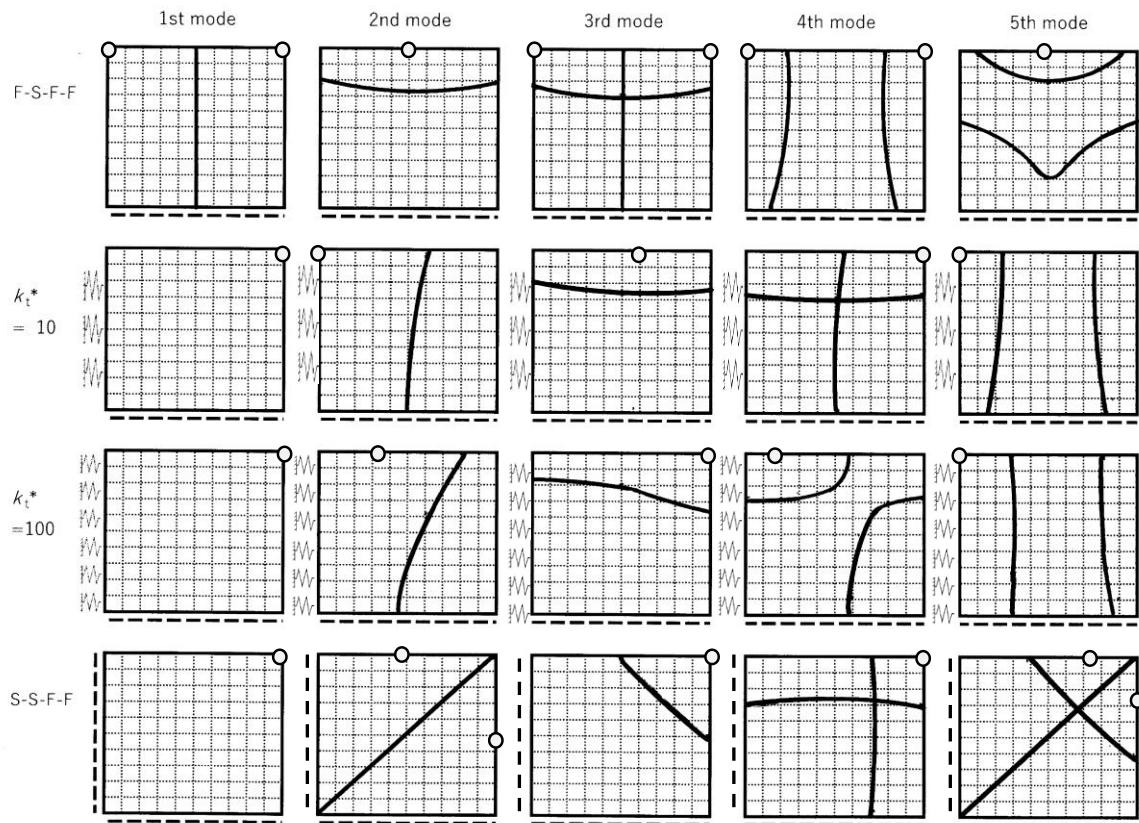


Figure 8. Mode shapes (nodal lines) of square plates (Ex.6)

3.4. Mode shapes of square plates

Elastic constraint on edges naturally affects mode shapes (nodal lines) of the plates, and as a representative case, Figure 8 shows effects of elastic constraint of the edge ($x=a/2$) in Ex.6. In the figure, translation spring and simple support along Edge(1) and Edge(2) are illustrated, respectively, in each plate. Nodal lines (lines of zero deflection) is plotted in curved solid thick lines and the location of maximum amplitude is denoted by a circle “○” in the figures.

The mode shapes of F-S-F-F, TS-S-F-F ($k_t^*=10$), TS-S-F-F ($k_t^*=100$) and S-S-F-F plates are presented in the first, second, third and fourth rows, respectively. For each value of k_t^* , the lowest five modes are presented, but one RBM is removed in F-S-F-F plate. It is seen that as the stiffness is increased from $k_t^*=0$ to $k_t^*=\infty$, nodal lines are skewed because constraint from Edge(1) makes asymmetric. It is also easily recognized that the nodal line pattern of 1st mode in the first row becomes 2nd mode in the second, third and fourth rows. Likewise, the nodal line patterns of 3rd and 4th in the first row are taken over to 4th and 5th modes, respectively, in the lower rows.

4. Conclusions

In the literature survey by this author, it was found that the reasonable amounts of natural frequencies are already obtained for rectangular plates with rotational springs on the edges, but those of plates with translational springs has received sparse treatment. To remedy this lack in frequency data, this paper attempted to calculate

frequencies by proposing a simple semi-analytical approach. Also a computation code by the finite element method was developed by the author.

Numerical examples cover rectangular plates from totally free plate to totally simply supported on all edges. Nine numerical examples are presented in terms of different degree of elastic constraints. Tables and figures are provided in the examples with different aspect ratios. The contour plots are given to demonstrate effects of translational spring on mode shapes,

It is hoped that these frequency data fill the existing gap and will be the useful structural design data involving plate components weakly coupled with supporting structure.

Acknowledgement

This author expresses his gratitude to the Japan Society for the Promotion of Science (JSPS) for the Funding Program MEXT/JSPS KAKENHI Grant Number 21K03957.

References

- [1] A. W. Leissa, *Vibration of Plates*. NASA-SP-160, 1969.
- [2] D. J. Gorman, *Vibration analysis of plates by the superposition method*. World Scientific Pub, 1999.
- [3] A. W. Leissa, “The free vibration of rectangular plates,” *J. Sound Vib.*, vol. 31, no. 3, pp. 257–293, 1973.
- [4] Y. Narita, “Combinations for the free-vibration behaviors of anisotropic rectangular plates under general edge conditions,” *J. Appl. Mech.*, vol. 67, no. 3, pp. 568–573, 2000.
- [5] Y. Narita, “Natural frequencies of rectangular plates in improved accuracy,” *EPI Int. J. Eng.*, vol. 5, no. 1, pp. 26–36, 2022.

- [6] P. A. A. Laura and E. Romanelli, "Vibrations of rectangular plates elastically restrained against rotation along all edges and subject to a bi-axial state of stress," *J. Sound Vib.*, vol. 37, no. 3, pp. 367–377, 1974.
- [7] C. E. Gianetti, L. Diez, and P. A. A. Laura, "Transverse vibrations of rectangular plates with elastically restrained edges and subject to in-plane, shear forces," *J. Sound Vib.*, vol. 54, no. 3, pp. 409–417, 1977.
- [8] P. A. A. Laura and R. Grossi, "Transverse vibration of a rectangular plate elastically restrained against rotation along three edges and free on the fourth edge," *J. Sound Vib.*, vol. 59, pp. 355–368, 1978.
- [9] P. A. A. Laura and R. Grossi, "Transverse vibrations of rectangular anisotropic plates with edges elastically restrained against rotation," *J. Sound Vib.*, vol. 64, pp. 257–267, 1979.
- [10] A. V. Bapat and Venkatramani, "Simulation of classical edge conditions by finite elastic restraints in the vibration analysis of plates," *J. Sound Vib.*, vol. 120, pp. 127–140, 1988.
- [11] D. J. Gorman, "A comprehensive study of the free vibration of rectangular plates resting on symmetrically-distributed uniform elastic edge supports," *J. Appl. Mech.*, vol. 56, no. 4, pp. 893–899, 1989.
- [12] R. O. Grossi and R. B. Bhat, "Natural frequencies of edge restrained tapered rectangular plates," *J. Sound Vib.*, vol. 185, no. 2, pp. 335–343, 1995.
- [13] K. M. Li and Z. Yu, "A simple formula for predicting resonant frequencies of a rectangular plate with uniformly restrained edges," *J. Sound Vib.*, vol. 327, no. 1–2, pp. 254–268, 2009.
- [14] W. L. Li, X. Zhang, J. Du, and Z. Liu, "An exact series solution for the transverse vibration of rectangular plates with general elastic boundary supports," *J. Sound Vib.*, vol. 321, no. 1–2, pp. 254–269, 2009.
- [15] S. A. Eftekhari and A. A. Jafari, "Accurate variational approach for the free vibration of variable thickness thin and thick plates with edges elastically restrained against translation and rotation," *Int. J. Mech. Sci.*, vol. 68, pp. 35–46, 2013.
- [16] H. Ahmadian and M. Esfandiari, "Boundary condition identification of a plate on elastic support," *Int. J. Acoust. Vib.*, vol. 19, no. 4, pp. 282–286, 2014.
- [17] Z. Wan, "Free vibration analysis of rectangular plates with arbitrary elastic boundary conditions," in *INCE Conference Proceedings, InterNoise21*, 2021, pp. 1891–1898.
- [18] J. Zhang *et al.*, "Free vibration analysis of thin rectangular plates with two adjacent edges rotationally-restrained and the others free using finite Fourier integral transform method," *Struct. Eng. Mech.*, vol. 80, no. 4, pp. 455–462, 2021.
- [19] B. Leng, S. Ullah, T. Yu, and K. Li, "New analytical free vibration solutions of thin plates using the Fourier series method," *Appl. Sci.*, vol. 12, no. 17, 2022.
- [20] Y. Narita, "Maximum frequency design of laminated plates with mixed boundary conditions," *Int. J. Solids Struct.*, vol. 43, no. 14–15, pp. 4342–4356, 2006.